Available online at www.sciencedirect.com
SCIENCE DIRECT®
Journal of Solid State Chemistry 178 (2005) 536–544
JOURNAL OF SOLID STATE CHEMISTRY
www.elsevier.com/locate/jssc

Spectrum analysis of U^{3+}-doped $LaBr_3$ single crystals. Part 1: crystal-field analysis

Marcin Sobczyk, Janusz Drożdżyński*, Mirosław Karbowiak

Faculty of Chemistry, University of Wrocław, ul. F. Joliot-Curie 14, 50-383 Wroclaw, Poland

Received 19 May 2004; received in revised form 8 October 2004; accepted 15 October 2004

Abstract

Single crystals of U^{3+}:$LaBr_3$ were grown by the Bridgman–Stockbarger technique. High-resolution polarized absorption spectra of the crystals were recorded at 4.2 K in the 4000–50,000 cm^{-1} range. Sixty-four experimental crystal-field energy levels of the U^{3+} ion were fitted to a semiempirical Hamiltonian employing free-ion, one-electron crystal-field as well as two-particle correlation crystal-field (CCF) operators with an r.m.s. deviation of 28 cm^{-1}. The performed analysis of the spectra enabled the determination of crystal-field parameters and assignment of the observed $5f^3 \rightarrow 5f^3$ transitions. The effects of selected CCF operators on the splitting of some specific U^{3+} multiplets have been investigated and the obtained values of Hamiltonian parameters are discussed and compared with those reported in previous analyses.

Keywords: Uranium(3+); Uranium tribromide; U(3+)-doped single crystals; Crystal-field; Energy levels; Crystal-field parameters; Correlation crystal-field parameters; Low-temperature absorption spectra

1. Introduction

The aim of the investigations has been the performance of a comprehensive spectroscopic analysis of U^{3+} ions doped in $LaBr_3$ single crystals. The first part of the analysis presents crystal-field calculations with the inclusion of two-particle correlation crystal-field (CCF) operators in order to obtain a reliable set of atomic and crystal-field parameters. The investigations of upconversion and luminescence properties of the crystals will be presented in the second part.

The first analysis of this system has been presented in the Ph.D. thesis of A.P. Paszek at the Johns Hopkins University in Baltimore [1]. For reasons unknown to us the results have not been published, with the exception of atomic and crystal-field parameters, presented in a review article by Carnall [2]. However, from this set of parameters we were not able to reproduce an energy level structure consistent with experimental data of the U^{3+} ion. Furthermore, since the first *f–d* bands in these crystals appear at about 21,000 cm^{-1} one may suspect that at least 20 from among the 117 crystal-field levels included in the calculations by Paszek, were of uncertain origin. Among the so far obtained U^{3+}-doped single crystals only $LaCl_3$ [3–5], $LaBr_3$ and $LiYF_4$ [6] exhibit a suitable site symmetry for precise energy-level tructure investigations with application of electric and magnetic–dipole transition selection rules. Crystal-field analyses of U^{3+}:Cs_2NaYBr_6 [7] single crystals as well as UCl_3 and UBr_3 polycrystalline samples are also available [8].

2. Experimental

Uranium(3+)-doped single crystals of $LaBr_3$ with nominal 0.1, 0.05 and 0.01 mol% uranium concentration were grown in silica ampoules by the Bridgman–Stockbarger method. $LaBr_3$ was synthesized from La_2O_3

*Corresponding author. Fax: +48 71 238 23 48.
E-mail address: jd@wchuwr.chem.uni.wroc.pl (J. Drożdżyński).

0022-4596/$ - see front matter © 2004 Elsevier Inc. All rights reserved.
doi:10.1016/j.jssc.2004.10.024

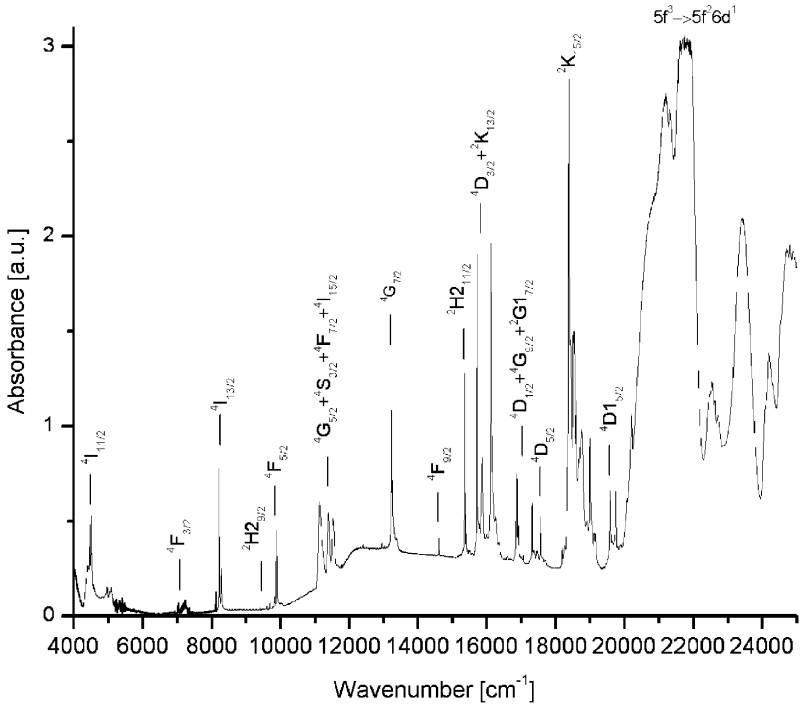

Fig. 1. Survey absorption spectrum of U^{3+}: $LaBr_3$ at 4.2 K.

(99.999%) by the ammonium bromide route and sublimed under high vacuum. Uranium tribromide was prepared according to the procedure reported in Ref. [9]. Polarized absorption spectra of the $LaBr_3$:U^{3+} single crystals were recorded on a Cary 5E NIR-Vis-UV spectrophotometer in the 4000–50,000 cm^{-1} range (Fig. 1). Luminescence spectra have been obtained upon excitation of the U^{3+} ions in this crystal by an argon ion laser (0.24 W at wavelength 514 nm, 19455 cm^{-1}). Luminescence was dispersed by a 1-m double-grating monochromator, detected by the Hamamatsu R-928 photomultiplier, averaged by the Stanford model SRS 250 boxcar integrator and stored in a PC computer. For low-temperature measurements a continuous flow helium cryostat (Oxford model CF 1204) equipped with a temperature controller was used.

3. Energy level calculations

Crystal-field calculations have been performed by applying the f-shell empirical program, delivered by M.F. Reid (University of Canterbury, New Zealand) and running on PC under the Linux Mandrake operating system. The effective operator model was used for the analysis of the obtained data [10]. The eigenvectors and eigenvalues of the crystal-field levels were obtained by a simultaneous diagonalization of the combined free-ion and crystal-field energy matrices. The applied Hamiltonian includes the following terms:

$$\hat{H} = \hat{H}_{\mathrm{A}} + \hat{H}_{\mathrm{CF}} + \hat{H}_{\mathrm{CCF}}. \tag{1}$$

The free-ion Hamiltonian $\hat{H}_{\mathrm{A}}$ [11] contains the isotropic (atomic) parts of $\hat{H}$ and is defined as

$$\begin{aligned}\hat{H}_{\mathrm{A}} = {} & E_{\mathrm{ave}} + \sum_{k=2,4,6} F^k(nf,nf)\hat{f}_k + \zeta_{5f}\hat{A}_{\mathrm{SO}} \\ & + \alpha\hat{L}(\hat{L}+1) + \beta\hat{G}(G_2) + \gamma\hat{R}(R_7) \\ & + \sum_{i=2,3,4,6,7,8} T^i\hat{t}_i + \sum_{j=0,2,4} M^j\hat{m}_j + \sum_{k=2,4,6} P^k\hat{p}_k \end{aligned} \tag{2}$$

where E_{ave} is the spherically symmetric one-electron part of the Hamiltonian, $F^k(nf,nf)$ and ζ_{5f} represent the radial parts of the electrostatic and spin–orbit interactions, while $\hat{f}_k$ and $\hat{A}_{\mathrm{SO}}$ are the angular parts of these interactions, respectively. The α, β *and* γ, parameters are associated with the two-body correction terms. $G(G_2)$ and $G(R_7)$ are Casimir operators for the G_2 and R_7 groups. L is the total orbital angular momentum. The three-particle configuration interaction is expressed by $T^i\hat{t}^i(i=2,3,4,6,7,8)$, where T^i are parameters and $\hat{t}_i$ are three-particle operators.

The electrostatically correlated spin–orbit perturbation is represented by the P^k parameters and those of the spin–spin and spin-other-orbit relativistic corrections by the M^j parameters. The operators associated with these parameters are designated by $\hat{m}^j$ and $\hat{p}^k$, respectively.

The $\hat{H}_{CF}$ term of the Hamiltonian represents the one electron crystal-field and is defined as [10]

$$\hat{H}_{CF} = \sum_{k,q,i} B_q^k C_q^{(k)}(i), \tag{3}$$

where $C_q^{(k)}(i)$ is a spherical tensor of rank k and B_q^k are crystal-field parameters. The crystal-field Hamiltonian for the C_{3h} site is expressed as follows:

$$H_{CF} = B_0^2 C_0^2 + B_0^4 C_0^4 + B_0^6 C_0^6 + B_6^6 (C_{-6}^6 + C_6^6) + B'^6_6 i(C_{-6}^6 + C_6^6). \tag{4}$$

Depending on an arbitrary choice of the coordinating system the B_6^6 parameter may be either complex, purely real or purely imaginary. In the coordinate system chosen in this analysis, the imaginary part of B_6^6 vanishes. The last term of the complete Hamiltonian represents the correlated two-electron crystal-field interactions. Following Reid [12] the parameterization of these interactions may be written in Judd's notation [13] as a set of G_{iQ}^K parameters:

$$\hat{H}_{CCF} = \sum_{i,K,Q} G_{iQ}^K \hat{g}_{iQ}^{(K)}, \tag{5}$$

where K runs through the even integers from 0 to 12, i distinguishes different $\hat{g}_{iQ}^{(K)}$ operators with identical K, and Q is restricted by the crystal field symmetry.

Since there appear, 41 additional independent parameters one cannot include all of them in a fit with a set of 64 experimental data only. In order to reduce the number of this CCF parameters we have followed the procedure presented by Li and Reid [14] in an analysis of some Nd^{3+}-doped crystals and we applied it in a recent analysis of U^{3+}:$LaCl_3$ [5] low-temperature absorption spectra. It has been shown that the inclusion of only a few of the parameters have markedly improved the fits and could resolve problems with poorly fitted levels by the one-electron crystal-field operator H_{CF}. In the performed spectrum analysis of U^{3+}:$LaBr_3$ the most problematic multiplets were $^2H2_{9/2}$ and $^4F_{5/2}$ for which a considerable discrepancy between the calculated and experimental splitting values has been found. Similarly, as in our previous analysis [5], we have stated that only the three $G_{10A,0}^4$, G_{10B0}^4 and G_{20}^4 fourth-rank parameters and one G_{10B0}^6 sixth-rank parameter were statistically significant.

$LaBr_3$ crystallizes in the UCl_3-type structure (space group $P6_3/m$, No. 176) with the C_{3h} point symmetry of the La^{3+} site [15]. The La^{3+} ions are coordinated by nine Br^- ions in the shape of a tricapped trigonal prism. The U^{3+} ions randomly substitute for La^{3+} site. No hints of clustering or the occupation of other lattice sites could be detected. The crystal field splits the atomic states of the $5f^3$ configuration into Kramers doublets which may be classified as having the $E_{1/2}(\Gamma_7 + \Gamma_8)$, $E_{3/2}(\Gamma_{11} + \Gamma_{12})$ or $E_{5/2}(\Gamma_9 + \Gamma_{10})$ symmetry in the C_{3h} double-rotation group. The selection rules for the

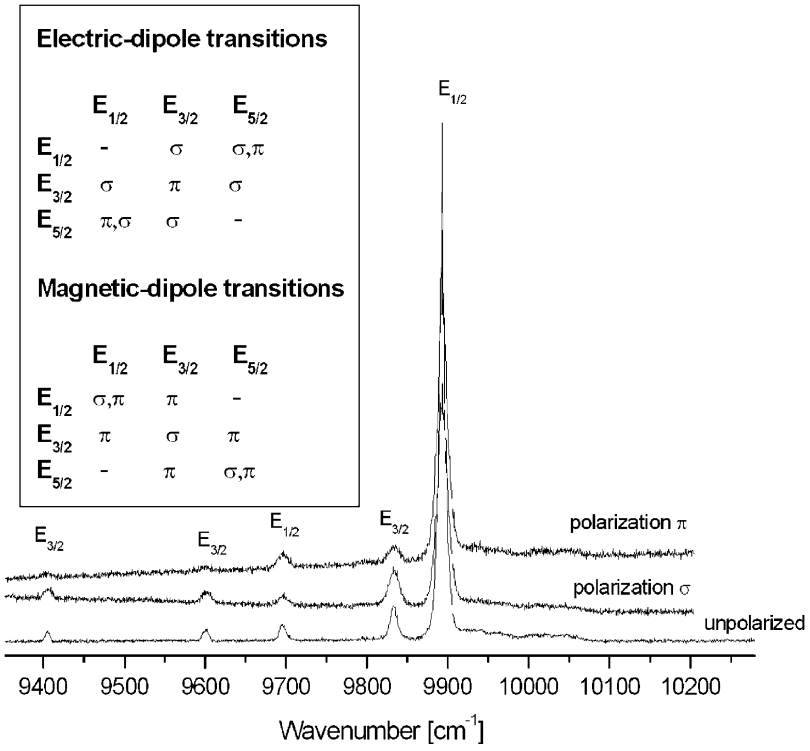

Fig. 2. Absorption transitions in π and σ polarization, from the $^4I_{9/2}$ ground state to the excited $^2H2_{9/2}$ and $^4F_{9/2}$ multiplets of the U^{3+}:$LaBr_3$ and U^{3+}:$LaCl_3$ single crystals. The insert gives selection rules for electric-dipole and magnetic-dipole transitions of U^{3+}:$LaBr_3$ (site symmetry C_{3h}). σ and π correspond to E⊥c and E || c, respectively.

electric–dipole and magnetic–dipole transitions are given in the insert of Fig. 2. The lowest crystal-field level of the ground $^4I_{9/2}$ multiplet manifold of U^{3+} has the $E_{5/2}$ symmetry. Since the transitions observed in liquid helium temperature originate only from this level they must terminate on the $E_{3/2}$ or $E_{1/2}$ excited level for σ polarization and $E_{1/2}$ for π polarization. Hence, the selection rules allow for an unambiguous assignment of the irrep labels of all lines observed in the spectrum. The incompletely diminished intensity of the forbidden transitions observed in Fig. 2 is probably caused by a small distortion of the C_{3h} symmetry of the U^{3+} ion.

In the fitting procedure, 64 experimental energy levels have been determined and assigned from 5 K unpolarized as well as σ- and π-polarized absorption spectra. The levels were fitted to the parameters of the phenomenological Hamiltonian (1). In the final fitting procedure 14 atomic parameter, 4 one-electron CF parameters and 4 CCF parameter were freely varied. The initial values of the free-ion and crystal field parameters were taken from the previous analyses [4,5]. The T^8 and M^0 parameters were kept at a constant value. The P^2 parameter was varied while P^4 and P^6 were kept at a constant ratio to P^2. For comparison we have also performed a fit without the CCF parameters. The complete parameter sets for both fits are presented in Table 1. The experimental and calculated energy level values are presented in Table 2. In the analysis performed by Paszek [1] of the U^{3+}:$LaBr_3$ absorption spectrum, were included 117 experimental crystal-field levels, positioned up to 25,723 cm^{-1}. Since, above 21,000 cm^{-1}, the *f–f* bands are obscured by strong and broad *f–d* bands, these results may not be considered as fully reliable.

In the calculations the complete (364×364) $SLJM_J$ matrix has been diagonalized. The quality of the fits were determined using the r.m.s. deviation (in cm^{-1}) defined as

$$r.m.s. = \sum \left(\frac{\left(E_{\exp.} - E_{calc}\right)^2}{(n-p)} \right)^{1/2}, \quad (6)$$

where n is equal to the number of levels and p is the number of parameters that are varied freely. In order to

Table 1
Hamiltonian parameters (in cm^{-1}) obtained from crystal-field (CF) and correlation crystal-field (CCF) analyses

Parameter[a]	U^{3+}:$LaBr_3$		UBr_3 [8]	U^{3+}:$LaCl_3$ [5]	U^{3+}:$LaBr_3$ [1]
	CF	CCF	CCF	CCF	CF
E_{avg}	19,313(56)	19,339(50)	19,213(60)	19,426(34)	
F^2	38,085(203)	38,528(180)	37,931(216)	38,459(128)	38,332
F^4	31,442(232)	31,732(209)	30,281(256)	30,786(161)	32,959
F^6	22,310(244)	22,416(217)	20,536(257)	19,981(174)	22,563
ζ	1620(15)	1621(13)	1606(16)	1614(11)	1602
α	29(7)	29(6)	29(7)	31(4)	29
β	−880(36)	−893(33)	−864(46)	−886(34)	−918
γ	1452(126)	1391(113)	1690(136)	1928(93)	[1200]
T^2	538(99)	426(87)	347(105)	388(68)	[380]
T^3	75(29)	56(23)	17(28)	39(22)	49
T^4	234(47)	250(42)	252(48)	154(33)	236
T^6	−55(63)	−159(52)	−303(64)	−233(38)	−419
T^7	496(53)	489(42)	292(50)	401(35)	369
T^8	[300]	[300]	[300]	[300]	(350)
M^0	[0.6720]	[0.672]	[0.672]	[0.672]	[0.67]
P^2	1411(71)	1330(62)	1616(76)	1491(52)	—
B_0^2	372(38)	373(33)	350(43)	312(33)	407
B_0^4	−220(66)	−207(68)	−562(78)	−459(66)	−539
B_0^6	−1252(61)	−1174(55)	−1568(69)	−1462(55)	−1226
B_6^6	797(52)	855(45)	770(54)	1027(47)	590
$G^4_{10A,0}$		926(96)	969(135)	1001(98)	
$G^4_{10B,0}$		307(90)	744(103)	484(91)	
$G^4_{2,0}$		1431(187)	793(207)	817(181)	
$G^6_{10B,0}$		−1454(109)	−1399(126)	−1590(108)	
N	64	64	46	67	117
r.m.s[b]	33	28	31	29	27

[a]The parameters are defined in Section 3. Values in brackets indicate parameter errors. Parameters in square brackets were kept constant during the fitting procedure. $P^4 = 0.75\ P^2$, $P^6 = 0.5\ P^2$.

[b]Standard deviation. See equation (6).

Table 2
Electronic states, symmetry labels, experimental and calculated energy levels of U^{3+}:$LaBr_3$

SLJ multiplet[a]	Irrep.	Det.[b]	CF			CCF	
			Exptl energy (cm^{-1})	Calc. energy (cm^{-1})	$E_{exp.} - E_{calc}$ (cm^{-1})	Calc. energy (cm^{-1})	$E_{exp.} - E_{calc}$ (cm^{-1})
$^4I_{9/2}$	$E_{5/2}$	L	0	49	−49	45	−45
	$E_{1/2}$	L	190	175	15	210	−20
	$E_{3/2}$	L	200	195	5	195	5
	$E_{5/2}$	L	367	372[c]	−5	343	24
	$E_{3/2}$	L	392	360[c]	32	362	30
$^4I_{11/2}$	$E_{3/2}$	A	4422	4424	−2	4426	−4
	$E_{1/2}$	A	4474	4455	19	4463	11
	$E_{5/2}$	L	4495	4506	−11	4495	0
	$E_{1/2}$	A	4514	4517	−3	4529	−15
	$E_{3/2}$	A	4522	4529	−7	4534	−12
	$E_{5/2}$	L	4575	4566	9	4559	16
$^4F_{3/2}$	$E_{1/2}$	A	7009	7005	4	7007	2
	$E_{3/2}$	A	7034	7030	4	7025	9
$^4I_{13/2}$	$E_{1/2}$	A	8114	8117	−3	8116	−2
	$E_{3/2}$	A	8181	8203	−22	8195	−14
	$E_{1/2}$	A	8213	8216	−3	8218	−5
	$E_{5/2}$			8252		8240	
	$E_{1/2}$	A	8260	8268	−8	8275	−15
	$E_{3/2}$			8307		8310	
	$E_{5/2}$			8369		8363	
$^2H2_{9/2}$	$E_{5/2}$			9469		9346	
	$E_{3/2}$	A	9406	9481	−75	9434	−28
	$E_{3/2}$	A	9600	9610[c]	−10	9612	−12
	$E_{1/2}$	A	9696	9588	108	9650	46
	$E_{5/2}$			9698		9670	
$^4F_{5/2}$	$E_{5/2}$			9829		9817	
	$E_{3/2}$	A	9833	9842	−9	9859	−26
	$E_{1/2}$	A	9893	9877	16	9866	27
$^4G_{5/2}+$	$E_{1/2}$	A	11086	11059	27	11047	39
$^4S_{3/2}+$	$E_{1/2}$	A	11129	11124[c]	5	11129	0
$^4F_{7/2}+$	$E_{3/2}$	A	11144	11121[c]	23	11134	10
$^4I_{15/2}$	$E_{5/2}$			11168		11160	
	$E_{3/2}$	A	11179	11184	−5	11184	−5
	$E_{1/2}$	A	11243	11227	16	11213	30
	$E_{3/2}$	A	11395	11423	−29	11404	−9
	$E_{5/2}$			11434		11409	
	$E_{1/2}$	A	11425	11444	−19	11442	−17
	$E_{5/2}$			11504		11505	
	$E_{1/2}$	A	11548	11506	46	11504	44
	$E_{3/2}$		11565	11559	6	11549	17
	$E_{5/2}$			11652		11616	
	$E_{1/2}$	A	11689	11676	13	11671	18
	$E_{3/2}$			11747		11737	
	$E_{3/2}$			11835		11822	
	$E_{5/2}$			11937		11920	
$^4G_{7/2}$	$E_{5/2}$	L	13142	13188	−46	13183	−41
	$E_{3/2}$	A	13217	13203	14	13210	7
	$E_{1/2}$	A	13238	13306[c]	−68	13298[c]	−61
	$E_{5/2}$			13248[c]		13245[c]	
$^4F_{9/2}$	$E_{5/2}$			14577		14535	
	$E_{1/2}$	A	14607	14595	12	14610	−3
	$E_{3/2}$	A	14622	14630	−8	14633	−11
	$E_{5/2}$			14648		14628	
	$E_{3/2}$			14665		14690	

Table 2 (*continued*)

SLJ multiplet[a]	Irrep.	Det.[b]	CF			CCF	
			Exptl energy (cm^{-1})	Calc. energy (cm^{-1})	$E_{exp.} - E_{calc}$ (cm^{-1})	Calc. energy (cm^{-1})	$E_{exp.} - E_{calc}$ (cm^{-1})
$^2H2_{1/2}$	$E_{1/2}$	A	15352	15330	22	15358	−6
	$E_{3/2}$	A	15362	15366	−4	15349	13
	$E_{1/2}$	A	15393	15417[c]	−24	15440[c]	−47
	$E_{3/2}$	A	15405	15391[c]	14	15374[c]	31
	$E_{5/2}$			15460		15372	
	$E_{5/2}$			15554		15466	
$^4D1_{3/2}$	$E_{1/2}$	A	15723	15757	−34	15749	−26
	$E_{3/2}$	A	15776	15762	14	15758	18
$^2K_{13/2}$	$E_{1/2}$	A	15863	15852	11	15844	19
	$E_{3/2}$	A	15994	16020[c]	−26	16003[c]	−9
	$E_{5/2}$			16010[c]		15965[c]	
	$E_{1/2}$	A	16023	16027	−4	16050	−27
	$E_{5/2}$			16074		16032	
	$E_{3/2}$			16094		16133	
	$E_{1/2}$			16132		16170	
$^4D_{1/2}$	$E_{1/2}$	A	16251	16264	−13	16246	5
$^4G_{9/2}+$	$E_{5/2}$			16734		16703	
$^2G1_{7/2}$	$E_{3/2}$	A	16796	16753	43	16758	38
	$E_{3/2}$	A	16807	16792	15	16794	13
	$E_{5/2}$			16849		16841	
	$E_{1/2}$	A	16870	16851	19	16837	33
	$E_{3/2}$	A	16886	16931[c]	−45	16916	−30
	$E_{1/2}$	A	16914	16914[c]	0	16920	−6
	$E_{5/2}$			17003		16981	
	$E_{5/2}$			17056		17029	
$^4D_{5/2}$	$E_{5/2}$			17257		17258	
	$E_{3/2}$	A	17322	17326	−4	17327	−5
	$E_{1/2}$			17330		17338	
$^2K_{15/2}$	$E_{1/2}$	A	18363	18356	7	18356	7
	$E_{3/2}$	A	18394	18396	−2	18405	−11
	$E_{1/2}$	A	18414	18458	−44	18443	−29
	$E_{3/2}$	A	18580	18550	30	18545	35
	$E_{5/2}$			18572		18556	
	$E_{1/2}$	A	18618	18604	14	18608	10
	$E_{3/2}$	A	18645	18641	4	18642	3
	$E_{5/2}$			18673		18669	
$^4D2_{3/2}$	$E_{1/2}$	A	19006	19004	2	19002	4
	$E_{3/2}$	A	19020	19014	6	19022	−2
$^2H1_{11/2}$	$E_{1/2}$	A	19600	19618	−18	19621	21
	$E_{3/2}$	A	19625	19643	−18	19643	−18
	$E_{1/2}$	A	19706	19659	47	19685	21

[a]Nominal spectroscopic symbols for the energy state(s) associated with the group of levels.
[b]Values determined from analysis of luminescence (L) or absorption (A) spectra.
[c]Indicate levels for which the order of the calculated values was reversed.

compare the magnitudes of the total crystal field strength the scalar parameter [16]

$$N_v = \left[\sum_{k,q} (B_q^k)^2 \frac{4\pi}{(2k+1)}\right]^{1/2} \quad (7)$$

has been applied.

4. Results and discussion

In the 4000–19750 cm^{-1} absorption range relatively sharp and well-separated bands of intraconfigurational $5f^3 \rightarrow 5f^3$ transitions have been observed (Fig. 1). At higher wave numbers the bands are obscured by strong $5f^3 \rightarrow 5f^2 6d^1$ transitions. Since the absorption spectrum is

similar to those of U^{3+}:$LaCl_3$ [5] and UBr_3 [8] a comparison of the spectra enabled an unambiguous identification of most of the recorded crystal-field bands. In Fig. 2, absorption transitions in π and σ polarization, from the $^4I_{9/2}$ ground state to the excited $^2H2_{9/2}$ and $^4F_{9/2}$ multiplets of the U^{3+}:$LaBr_3$ and U^{3+}:$LaCl_3$ single crystals are presented. One may observe an expected red shift and a somewhat smaller crystal-field splitting of the bands with reference to those of U^{3+}:$LaCl_3$. It is worth noting, however, that the crystal-field splitting of the $^2K_{13/2}$ as well as of some other multiplets, located at higher energies, exhibit for the bromide crystal somewhat larger values (Table 3). This irregularity may be attributed to the proximity of the *f–d* states, which in U^{3+}:$LaBr_3$ appear at lower wave numbers. A similar observation have been noticed by Lüthi et al. [17] in an analysis of Er^{3+}-doped $Cs_3Lu_2Cl_9$, $Cs_3Lu_2Br_9$ and $Cs_3Y_2I_9$ single crystals.

A comparison of the values of the total splitting and the centers of gravity of the LSJ multiplets, observed in the low-temperature spectra of U^{3+}:$LaCl_3$ and U^{3+}:$LaBr_3$, is presented in Table 3. The energy values of the crystal-field components of the $^4I_{9/2}$ ground level have been determined from an analysis of the emission spectra originating from the $^2K_{15/2}$, $^2H2_{11/2}$ and $^4F_{9/2}$ levels (Fig. 3, Table 2)

The largest E_{calc}–$E_{obs.}$ differences equal to -75 and $108\,cm^{-1}$ exhibit the recorded at 9406 and $9696\,cm^{-1}$ levels of the $^2H2_{9/2}$ multiplet, respectively. The order of the calculated value of the second one was reverse (see Table 2.). After inclusion of the CCF parameters the order became correct, the ($E_{exp.}$–$E_{calc.}$) values decrease down to 28 and $46\,cm^{-1}$ respectively, and the standard deviation for the overall fit decreases from 33 to $28\,cm^{-1}$

Most values of the Hamiltonian parameters obtained in this analysis (Table 1) are generally similar to those reported in our previous analysis of U^{3+}:$LaCl_3$ [4] and UBr_3 [6]. One may notice somewhat larger values for the F^k parameters and almost the same for ζ_{5f} with reference to those of U^{3+}:$LaCl_3$ and UBr_3. Besides, one observes significant differences in the values of γ and some of the three-body T^k parameters. An increase in metal-ligand covalency results in an increase of the average distance between the valence electrons, which in turn leads to a decrease of the Coulomb repulsion. At the same time the delocalization of the electron density leads to a reduction of the orbital angular momentum and consequently to a decrease of the spin–orbit coupling values. Thus, smaller values of the F^k and ζ parameters should be expected for U^{3+}:$LaBr_3$, which remain in disagreement with the results of our calculations. However, one should emphasize, that also in a crystal-field analysis of Er^{3+} ions diluted in $Cs_3Lu_2Cl_9$, $Cs_3Lu_2Br_9$ and $Cs_3Y_2I_9$ single crystals, the obtained values of the F^k parameters do not exhibit an expected steady decrease along the Cl–Br–I series of compounds [17]. We have attributed a similar inconsistency, noticed for the F^4 parameter in the CF analysis of U^{3+}:$Cs_3Lu_2Cl_9$ and U^{3+}:$Cs_3Y_2I_9$ single crystals [18] to uncertainties in the determination of the configuration interaction as well of some minor atomic parameters. Hence, it appears, that for the observed discrepancy in this analysis, similar factors may be responsible. Since, between U^{3+}:$LaCl_3$ and U^{3+}:$LaBr_3$ the values of the "free ion" parameters should not exhibit considerable

Table 3
A comparison of the total splittings and centers of gravity (CG) of LSJ multiplets in the low temperature spectra of U^{3+}:$LaCl_3$ and U^{3+}:$LaBr_3$ single crystals

LSJ multiplet	Total splitting		CG relative	
	U^{3+}:$LaCl_3$ (cm^{-1})	U^{3+}:$LaBr_3$ (cm^{-1})	U^{3+}:$LaCl_3$ (cm^{-1})	U^{3+} :$LaBr_3$ (cm^{-1})
$^4I_{9/2}$	451	392	269	230
$^4I_{11/2}$	164	153	4540	4450
$^4F_{3/2}$	18	25	7090	7021
$^4I_{13/2}$	285	249	8279	8240
$^2H2_{9/2}$	383	324	9595	9544
$^4F_{5/2}$	90	76	9912	9848
$^4G_{5/2}+{}^4S_{3/2}+{}^4F_{7/2}+{}^4I_{15/2}$	968	834	11498	11445
$^4G_{7/2}$	111	103	13298	13210
$^4F_{9/2}$	187	156	14686	14616
$^2H2_{11/2}$	159	114	15455	15392
$^4D1_{3/2}$	56	53	15853	15749
$^2K_{13/2}$	270	307	16117	16026
$^4D_{1/2}$	0	0	16518	16251
$^4G_{9/2}+{}^2G1_{7/2}$	334	326	16941	16870
$^4D_{5/2}$	73	80	17546	17329
$^2K_{15/2}$	298	306	18666	18530
$^4D2_{3/2}$	12	14	19209	19013

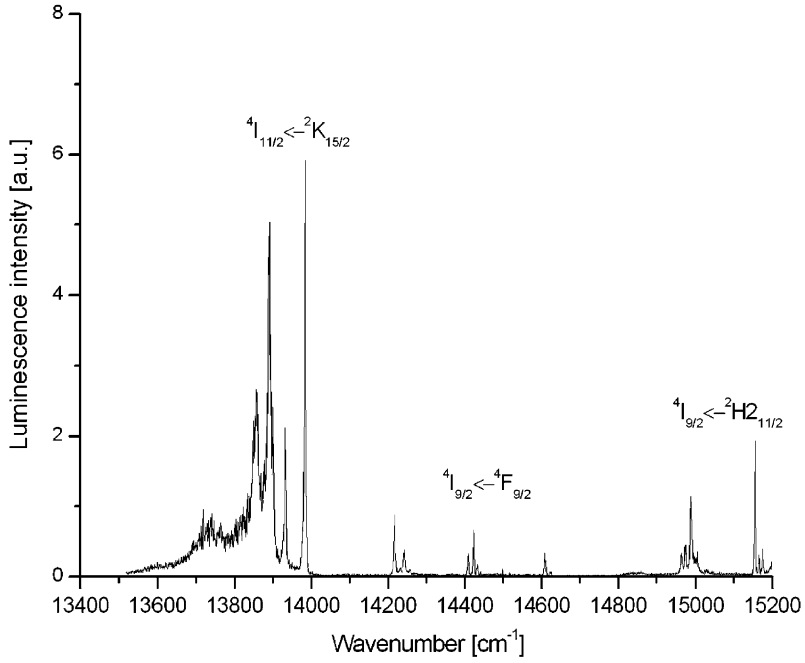

Fig. 3.

changes, one may assume that those which display such differences, e.g. γ and most of the three-body T^k parameters, have not been correctly determined. An additional important factor responsible for the discrepancy, appear to be the influence of excited configurations, evidenced by the above-mentioned larger CF splitting of U^{3+}:$LaBr_3$ multiplets, located at higher wavenumbers. Since the applied Hamiltonian is representing the combined free-ion and CF interactions this influence is not separately taking into consideration in the calculations. Hence, some deficiencies in the CF part may be absorbed by the free-ion part, resulting in the appearance of disturbed values of the, e.g. F^k parameters, and vice versa.

The one-electron B_q^k parameter values are, as expected for a bromide system, somewhat smaller than those of U^{3+}:$LaCl_3$ and UBr_3 with the exception of B_0^2 with reference to U^{3+}:$LaCl_3$ and UBr_3, and B_6^6 with reference to UBr_3. The values of the CCF parameters are similar to those determined for $LaCl_3$, except of $G_{2,0}^4$, which assumed a considerably larger value.

For comparison purposes, the B_q^k values should be multiplied by $\sim 14 \times (12/77)^{1/2}$ due to a differently normalization of the CCF operators. The values of the $G_{10A,0}^4/B_0^4$, $G_{10B,0}^4/B_0^4$, G_2^4/B_0^4 and $G_{6A,0}^6/B_0^6$ ratios calculated in this manner are equal to -0.81, -0.27, -1.25 and 0.22, respectively. Thus, the fourth-rank CCF parameters achieve the same order of magnitude as the one-electron parameters. The corresponding ratios for U^{3+}:$LaCl_3$ are equal to -0.39, -0.19, -0.32 and 0.20, and are larger than those of the Nd^{3+}:$LaCl_3$ crystals, for which the average corrected $G_{10A,0}^4/B_0^4$ ratio is about –0.1 [19]. This may point to a stronger correlation effect in the bromide crystal, but it may also result from a deficiency of the applied theoretical model for a description of CF levels of the $5f^3$ configuration. Hence, the observed improvement in the adjustment of some of these levels may result from the inclusion of additional parameters, which just on these levels display the largest influence.

The crystal-field of U^{3+}:$LaBr_3$ is somewhat weaker than those of UBr_3 or U^{3+}:$LaCl_3$, due to the comparatively long La–Br distances which causes that the particular multiplets are relatively well separated and, except of two, do not overlap. In accordance with this statement, the N_v total crystal-field strength parameter (7) for U^{3+}:$LaBr_3$ amount to $1593\,cm^{-1}$ (largest total splitting value $\Delta = 392\,cm^{-1}$) and is as expected smaller than that for UBr_3, ($N_v = 1923\,cm^{-1}$, $\Delta = 411\,cm^{-1}$) and U^{3+}:$LaCl_3$ ($N_v = 1904\,cm^{-1}$, $\Delta = 451\,cm^{-1}$.

5. Conclusion

The paper presents a comprehensive crystal-field energy level analyses of polarized low-temperature absorption spectra of U^{3+}:$LaBr_3$ single crystals. The analysis enabled the assignment of the observed $5f^3 \rightarrow 5f^3$ transitions and the determination of atomic and crystal-field parameters. Including contributions from two-electron correlation crystal-field interactions we could eliminate major discrepancies between the calculated and observed energy levels within the $^2H2_{9/2}$ multiplet.

The values of the obtained Hamiltonian parameters are discussed and compared with those reported in previous analyses. The obtained F^k parameters are somewhat larger with reference to those of U^{3+}:$LaCl_3$, which seems to result from difficulties in a correct determination of the configuration interaction and of some minor atomic parameter values. The CF splitting of multiplets located at higher than 16,000 cm^{-1} are unexpectedly larger for U^{3+}:$LaBr_3$ than for U^{3+}:$LaCl_3$, which may be attributed to the influence of the proximity of the opposite parity $5f^26d^1$ configuration.

Acknowledgments

This work was supported by the Polish Committee for Scientific Research within the Project No. 7TO9A080 20 as well as by the grant No. 2530/w/WCH/04 of the University of Wrocław, which is gratefully acknowledged.

References

[1] P. Paszek, Ph.D. Dissertation, The Johns Hopkins University, Baltimore, 1978.
[2] W.T. Carnall, Absorption and luminescence spectra, in: Gmelin Handbook of Inorganic Chemistry, Uranium Supplement, vol. A5, Springer, New York, pp. 69–161.
[3] H.M. Crosswhite, H. Crosswhite, W.T. Carnall, A.P. Paszek, J. Chem. Phys. 72 (1980) 5103.
[4] W.T. Carnall, Systematic analysis of the spectra of trivalent actinide chlorides in D_3h site symmetry, ANL Report 89/39.
[5] M. Karbowiak, J. Drożdżyński, M. Sobczyk, J. Chem. Phys. 117 (2002) 2800.
[6] E. Simoni, M. Louis, J.Y. Gesland, S. Hubert, J. Lumin. 65 (1995) 153.
[7] M. Karbowiak, E. Zych, P. Dereń, J. Drożdżyński, Chem. Phys. 287 (2003) 365.
[8] M. Sobczyk, M. Karbowiak, J. Drożdżyński, J. Solid State Chem. 170 (2003) 443.
[9] E. Zych, J. Drożdżyński, Polyhedron 9 (17) (1990) 2175.
[10] B.G. Wybourne, Spectroscopic Properties of Rare Earths, Interscience, New York, 1965.
[11] W.T. Carnall, G.L. Goodman, K. Rajnak, R.S. Rana, J. Chem. Phys. 90 (1989) 3443.
[12] M.F. Reid, J. Chem. Phys. 87 (5) (1987) 2875.
[13] B.R. Judd, J. Chem. Phys. 66 (1977) 3163.
[14] C.L. Li, M.F. Reid, Phys. Rev. B 42 (1990) 1903.
[15] K. Krämer, T. Schleid, M. Schulze, W. Urland, G. Meyer, Z. Anorg. Allg. Chem. 575 (1989) 61–70.
[16] F. Auzel, O.L. Malta, J. Phys. (France) 44 (1983) 201.
[17] S.R. Lüthi, H.-U. Güdel, M.P. Hehlen, J. Chem. Phys. 110 (1999) 2033.
[18] M. Karbowiak, A. Mech, J. Drożdżyński, W. Ryba-Romanowski, M.F. Reid, J. Phys. Chem. B, in press.
[19] C.L. Li, M.F. Reid, Phys. Rev. B 42 (1990) 1903.